

CADMIUM REMOVAL FROM AQUEOUS SOLUTION BY NA-P ZEOLITE SYNTHESIZED FROM COAL FLY ASH

¹PayalJain,²Suresh Jain and ³M.K.Dwivedi

^{1,3}Department of Chemistry, Government.HolkarScience College Indore (M.P)

²Government Degree College DhanupurHandia,Allahabad,(U.P)

pjain2308@gmail.com, jainsuresh6730@gmail.com, dwivedimk12@gmail.com

Abstract

Direct hydrothermal treatment method was employed to synthesize zeolite from coal fly ash with sodium hydroxide at different concentration ratios at varying temperatures of 350,450 and 550 °C with activation time of 12 hr. Characterization of coal fly ash and of synthesized zeolite was done using XRF,XRD, FTIR and SEM. Adsorption of Cd(II) ion has been studied and the adsorption capacity of zeolite has been determined. The results of batch studies revealed that the adsorption of Cd(II) was strongly pH dependent and maximum Cd(II) removal was obtained at equilibrium pH of 5.0. Optimum adsorbent dose and contact time were observed to be 10 g/l and 90 minutes respectively. Experimental data were analysed using Langmuir, Freundlich, Dubinin–Radushkevich (D-R) and Temkin. It was found that the adsorption equilibrium of Cd(II) on zeolite was best described by Langmuir isotherm($R^2=0.995$). The experimental results of this study clearly demonstrate that zeolite is suitable for adsorption of cadmium from aqueous solution.

Keywords: Cadmium, Fly ash, Na-P Zeolite, Isotherms, kinetics

Introduction

Among the various pollutants the discharge of heavy metal bearing waste is a matter of great concern. Toxic metals are introduced into the water sources through wastewater from different industries like metal plating, mining, pigment, battery, distillery, fertilizer, cement, etc. Cadmium is most toxic heavy metal present in water bodies; diseases like hypertension, muscular cramp, and osteoporosis are very common in occurrence further severity may lead to kidney damage, lung cancer etc¹⁻². Hence systematic study of the removal of cadmium from wastewater is inevitable from an environmental point of view..

A number of technologies have been developed for the removal of heavy metal ions from wastewater. These are ion exchange, solvent extraction, reverse osmosis, precipitation and adsorption. Among these adsorption is an important means for controlling the extent of pollution. Activated carbon adsorption is a well-known method for the removal of heavy metals³⁻⁵, but the high cost of activated carbon restricts its large-scale use for the abatement of heavy metal pollution in developing countries. Previously lot of researchers have used different adsorbents, developed from various industrial waste materials, for the removal of heavy metals, such as synthesising activated carbon from waste rice husk, waste plastics, use of natural zeolites etc.⁶⁻⁹ Still a low cost and efficient adsorbent is needed for the removal of cadmium metal ion from wastewater. Zeolites were found to exhibit good adsorption ability and cation exchange affinity for adsorbates particularly divalent ion. It has been reported that natural zeolite holds good potential for the adsorption of several heavy metal cations, e.g.Mn,Zn,Cu and Co and this could be used as alternative for activated carbon.¹⁰

Coal fly ash is a waste obtained from thermal power plants and is found in abundance throughout the world. Much research is being conducted on the use of waste materials in order to either prevent an increasing toxic threat to the environment or to streamline present waste disposal techniques by

making them more affordable. It, therefore, follows logically that an economically usable solution to this problem should include utilization of waste materials in new products for other applications rather than disposal in a landfill.

One of the promising areas in this context is synthesis of zeolites from the coal fly ash. The aluminosilicate glass in coal fly ash is a rich available source of Al and Si for zeolite synthesis so as to obtain high value industrial products with environmental utilization.¹¹ Several studies have been carried out on the synthesis of zeolite from coal fly ash by hydrothermal treatment.¹²⁻¹⁵ It is therefore important to study synthesis of zeolite from coal fly ash from various sources, as applications of zeolite is strongly influenced by the particle morphology, pore size and architecture and the type of channels. Therefore in order to improve functional performance of different kinds of zeolites, many studies were performed to improve synthetic approach to control pore channel system and morphology.

In this paper, efforts have been made to synthesize zeolite from coal fly ash for the removal of cadmium metal ion from aqueous solution. Cadmium was chosen due to its toxic nature and also due to very few studies has been reported for the removal of cadmium metal from zeolite synthesized from coal fly ash.

Materials and Methods

Sampling and Sample Pre-treatment: Coal fly ash was collected from H.E.G. Thermal Power Station, Mandideep (Bhopal) India. The sample was sealed and transported in airtight polythene bag and then air dried for 24 h. Before use, they were screened by 100micron sieve followed by removal of magnetic materials mainly iron fillings using a magnet which interfere in zeolite formation.

Cd(NO₃)₂ was used from MerkCo.. Stock solution of 1000mg/L was prepared in distill water, NaOH or HCl was used to adjust the initial pH, all the chemical reagents were of analytical grade.

Zeolite Synthesis: Several direct hydrothermal methods were applied for the synthesis of zeolite due to fast, economic and less involving than the other fusion and the microwave methods.¹⁶⁻¹⁹ Sodium hydroxide is added in different ratios of 1:1.2, 1:1.5 and 1: 2 with coal flyash and kept for fusion at varying temperatures of 350,450 and 550°C for 12 hours. Then washed off excess of alkali fusion mixtures with double distilled water and agitated for 24 hours on magnetic stirrer, filtered on whatmann filter paper and dried in oven for 12 hours at 110°C and stored in desiccators before use.

Characterization of Coal Fly Ash and Zeolite: The chemical constituents of fly ash were analyzed using Bruker S-8 Tiger WDXRF. The surface area was measured with a model QS-7 Quantasorb surface area analyzer. The specific gravity was determined using specific gravity bottles. The Scanning Electron Microscopy (SEM) was carried out using model LEO 438 VP, UK to study micro structure and qualitative characteristics of the ash of the fly ash. The identification of the mineralogical constituents and phase properties of fly ash was examined by Bruker D-8 advance X-ray diffractometer with a Cu-anode. The diffractometer was operated at 40 kV and 40 mA for 1 h over the range of 2θ from 0° to 80°. The infrared spectrum of the adsorbent was recorded in potassium bromide and Nujol mull in the range of 500-4000⁻¹cm using a Perkin Elmer spectrophotometer.

Sorption method: Batch experiments were performed for the determination of equilibrium time and the selection of isotherm conditions. Double distilled water sample (20 ml) of known concentration (100-500 mg/l) and pH with desired adsorbent dosage were agitated until the equilibrium was attained. pH value of aqueous solution of adsorbate was adjusted with either dilute HCl or NaOH solution to a constant value. The equilibrium adsorption uptake and percentage removal of adsorbate from the aqueous solution q_e (mg/g) was determined using the following relationship

$$\text{Amount adsorbed } q_e = \frac{(C_0 - C_e)V}{W} \quad (1)$$

$$\text{And \% removal } q_e = \frac{100(C_0 - C_e)}{C_0} \quad (2)$$

Where, C_0 is initial adsorbate concentration (mg/l), C_e is equilibrium adsorbate concentration (mg/l), V is the volume of solution (l), W is the mass of adsorbent (g)

The fly ash dose was varied from 0.1 to 0.5 g per 20 ml. The effect of pH was studied ranging from 4 to 10. After the required contact time, the solution was centrifuged. The residue concentration in centrifuged was determined by AAS.

Equilibrium Adsorption Isotherm Models: The adsorption isotherm particularizes the interaction of cadmium ion with an zeolite and is critical in optimizing the use of adsorbent. Adsorption equilibrium studies are carried out to correlate the adsorption capacity (q_e , $\text{mg}\cdot\text{g}^{-1}$) and residual adsorbate concentration (C_e , $\text{mg}\cdot\text{L}^{-1}$) in the liquid phase.²⁰⁻²¹ Thus it is essential to apply various isotherm models, i.e., Langmuir²², Freundlich²³, Dubinin–Radushkevich (D-R)²⁴, and Temkin²⁵, to find an accurate relationship between metal ion in the liquid and solid phase due to complex adsorption system is in liquid phase.

The Langmuir isotherm model is used to establish the relationship in monolayer coverage of adsorbate molecules.²⁶⁻²⁷ Model also assumes that homogeneous active sites exist at the surface of an adsorbent and that there are no interactions between two adsorbed species.

$$\frac{1}{q_e} = \frac{1}{q_m} + \frac{1}{b \cdot q_m} \cdot \frac{1}{C_e} \quad (3)$$

Where b is the Langmuir constant (intercept/slope), and q_m is the maximum adsorption capacity ($\text{mg}\cdot\text{g}^{-1}$) i.e., $1/\text{intercept}$; both can be calculated from the plot $1/q_e$ vs $1/C_e$. Moreover, C_e ($\text{mg}\cdot\text{L}^{-1}$) is the equilibrium adsorbate (Cd^{+2}) concentration in solution, and q_e ($\text{mg}\cdot\text{g}^{-1}$) is the equilibrium adsorbent Na-P zeolite capacity. Further analysis of the Langmuir model can be performed using the dimensionless equilibrium parameter²⁸, which is also called the separation factor.²⁹

$$R_L = \frac{1}{1 + K_L C_0} \quad (4)$$

R_L is the dimensionless constant which indicates the favorability of the adsorption process.

The Temkin isotherm model postulates are as follows: (i) the heat of adsorption of the surface molecules decreases linearly rather than logarithmically with coverage,³⁰ (ii) the adsorption process

is characterized by a uniform distribution of binding energies at the adsorbent surface,³¹ and (iii) this model covers the adsorbate-adsorbent interaction. The nonlinear form of Temkin model is given below.

$$q_e = \frac{R_T}{B_T} \ln(A_T C_e) \quad (5)$$

This equation can be liberalized as:

$$q_e = B_T \ln A_T + B_T \ln C_e \quad (6)$$

Where $B_T = \frac{RT}{bT}$, and T and R are absolute temperature (K) and the universal gas constant (8.314 J·mol⁻¹·K⁻¹), respectively.

The heat of adsorption decreases in magnitude with increasing adsorption for most of the adsorption systems.³² This behaviour is well considered by the Freundlich isotherm, previously known as an empirical isotherm. The Freundlich isotherm also considers that the pollutant undergoes adsorption onto the heterogeneous adsorbent. For solute adsorption from solution, the Freundlich isotherm is described as follows:

$$q_e = K_F C_e^{1/n} \quad (7)$$

where K_f and $1/n$ indicate the relative adsorption capacity and the heterogeneity factor, respectively.

The D-R isotherm was also used to analyze the equilibrium data.³³⁻³⁵ This model was neither considers homogenous surface assumption nor the constant potential of adsorption.

$$\ln q_e = \ln q_{DR} - \beta \varepsilon^2 \quad (8)$$

Where q_{DR} is the theoretical monolayer sorption capacity (mg·g⁻¹), and β is the constant of adsorption energy (mol²·KJ⁻²).

Adsorption Kinetics: To determine the rate of adsorption, experiments regarding the adsorption kinetics were performed as adsorption is a time dependent process. It is necessary to know the rate of adsorption for the design and evaluation of a treatment system. Kinetic experiments were carried out by varying the initial adsorbate concentration, i.e., 25, 75, and 100 mg·L⁻¹ over variable time steps.

Specific Rate Constant of Adsorption: The rate constant of adsorption for various adsorbate is determined from the following first order rate expression given by Lagergren equation.

$$\log (q_e - q_t) = \log q_e - \frac{K_{ad}}{2.303} t \quad (9)$$

Where q and q_e are amounts of metal adsorbed (moles/g) at time (t) and at equilibrium respectively and K_{ad} is the rate constant for adsorption (min⁻¹). A straight line plot of $\log (q_e - q_t)$ versus (t) suggested the applicability of Lagergren equation. The rate constant of adsorption (K_{ad}) was calculated from the slope of the plot.

The pseudo-second-order kinetic equation is described as:

$$\frac{t}{qt} = \frac{1}{k_2 q_e^2} + \frac{1}{q_e} t \quad (10)$$

Where k_2 (g/mg min) is the rate constant and q_e and q_t (mg/g) are the amount of Cu adsorbed on the Na-P Zeolite at equilibrium and at time t (min), respectively.

Intra particle Diffusion: To study the diffusion mechanism of adsorption, the kinetic results were evaluated using the intraparticle diffusion model. During the process, the adsorbate species are most probably transferred from the bulk of the solution into the solid phase.

The intraparticle diffusion equation is given as:

$$q_t = K_i t^{1/2} + C \quad (11)$$

Where K_i (mg/g min^{1/2}) is the intraparticle diffusion rate constant and C is the intercept. q_t and t has the usual meanings. The boundary layer thickness is described by the values of the intercept. The larger the intercept value, the greater is the boundary layer effect.

Elovich model: Elovich equation is applied successfully to describe second order kinetics assuming that the actual solid surfaces are energetically heterogeneous, but the equation does not favours any definite mechanism for adsorbate–adsorbent. It has extensively been accepted that the chemisorption process can be described by this semi-empirical equation. The linear form of this equation is given by:

$$q_t = \frac{1}{\beta} \ln \alpha \beta + \frac{1}{\beta} \ln t \quad (12)$$

Where α is the initial adsorption rate (mg/g min), and the parameter β is related to the extent of surface coverage and activation energy for chemisorption (g/mg).

Result and Discussion

Characterization of Fly ash and Zeolite:

X Ray Fluorescence: The chemical composition of Coal Fly Ash is shown in Table 1. Study reveals that it contains a total percentage of SiO_2 , Fe_2O_3 and Al_2O_3 of more than 80% and CaO of less than 20% this type of CFA used in this study can be classified as class F. The Coal Fly Ash contains mainly SiO_2 , Al_2O_3 ratio of 2.43:1. The fly ash predominantly consists of trace metals with the chief constituents being aluminosilicates, oxides and silicates of calcium, iron and other bases. These oxides have a tendency to form metal hydroxide complexes in the solution and the subsequent basic or acidic dissociation of these complexes at the solid-solution interface causes the development of a negative or positive charge on the surface.

XRD: X-ray Diffraction revealed the occurrence of the characteristic reflection peaks of CFA and the generated zeolite material (Figure 1-2). As shown in Figure 1, the XRD pattern of CFA mainly shows the presence of crystalline quartz and mullite phases. Ash is primarily composed of amorphous material besides some crystalline phases (mullite, hematite, quartz etc). The intensity of quartz is very strong with mullite forming a chemically stable and dense glassy surface layer. Whereas low calcium oxide intensity is characteristic of low-Ca Class-F fly ash. After CFA treatment several sharp diffraction peaks of high intensity emerge confirming formation of zeolites (Figure 2). Data obtained from XRD shows that the quartz and mullite have changed their mineral phases which is reflected by their intensity count/seconds. Zeolite from alkali activated flyash (1:1.5) was identified as Na-P type as confirmed by JCPDF software, corresponding to maximum

peak intensity of 390 counts per second and diffraction angle (2 theta) equal to 28° . It is observed that due to its alkali activation there is reduction in the silica and alumina contents associated with the crystalline particles of the flyash. This can be accredited to the dissolution of the metal oxides and release of corresponding soluble ions Na^+ . The Si/Al ratio of the zeolite crystals present in alkali activated flyash is around one, which corresponds to a tetrahedral framework structure of the zeolite Na-P where there is presence of the Al^{3+} which have replaced equal number of Si^{4+} . Hence, it can be considered that such replacement of ions results in development of negative charge in the tetrahedral framework from $(\text{SiO}_4)^{-4}$ to $(\text{AlO}_4)^{-5}$. This can be result of development of negative charge on the pores and channels of zeolite structure and external linkages of Na^+ to neutralize it in the tetrahedral framework consisting of Al^{3+} ions. The mullite phase did not change much, indicating that it was a relatively stable phase during the hydrothermal reaction.

FTIR: The infrared spectrum of fly ash (Figure 3) shows broad and weak peaks in the region of $4000\text{-}500\text{ cm}^{-1}$ which are associated with the functional groups that are on the surface of coal fly ash. The band appearing at 560 cm^{-1} is associated with octahedral aluminium present in mullite. Along with the, bands appearing between $800\text{-}600\text{ cm}^{-1}$ are associated with tetrahedral vibrations formed which are known as secondary building units and fragments of alumino-silicate system. Band appearing at 2360 cm^{-1} could be due to alkyl groups that are present in clay material of coal fly ash. Bands appearing at $800\text{-}1200\text{ cm}^{-1}$ and $450\text{-}550\text{ cm}^{-1}$ assign to asymmetric stretching mode and bending mode of T-O bond respectively. These bands are more or less dependent on the crystal structure. The mid infrared region of the spectrum contains the fundamental framework vibrations of $\text{Si}(\text{Al})\text{O}_4$ groupings. Although some interference can be made about surface functional groups from IR spectra but, the weak and broad bands do not provide any definitive information about the nature of the surface oxides. The data surely, indicate the presence of some surface groups on the CFA.

Observations show that there are significant changes in the intensities and the width of various bands due to interaction of flyash with alkali (Figure 4). It can be noticed that there is an increase in intensity and broadness of the stretching frequency OH band at 3452 cm^{-1} after the treatment. This is due to an increase in hydrated products due to the reaction between amorphous silicate and the alkali. Further the shift in the frequency to lower values indicates change in acidic character of the terminal Si-OH group. Moreover, asymmetrical stretching of TO_4 (SiO_4 and AlO_4) band corresponding to the variation in frequency from 1076 to 1000 cm^{-1} and the increase in its sharpness confirms synthesis of silicates and change in its acidic characteristics. This can be attributed to substitution of Si^{4+} by Al^{3+} in some of the tetrahedral framework of the primary building units of the aluminosilicates and their external linkage with the Na^+ ions due to their interaction with the alkali. The band at 434 cm^{-1} indicates the increased crystallization of product.

SEM analysis: The results of SEM investigation of coal fly ash and zeolite are shown in (Figure 5-6). Figure 5 reveals typical fly ash morphology and surface texture. Most of the particles present in the fly ash are sub-angular and spherical in shape. The image also shows that the particles present in the fly ash are covered with relatively smooth grains of quartz, clusters of iron (Fe-oxide). Irregular surface of glass matrix so observed may be outcome of an increase in adsorbent pore volume.

Figure 6 shows a significant transition in morphology from lumps to crystalline form which is attributed to chemical reaction between Si^{4+} , Al^{3+} , and Na^+ ions and their nucleation and precipitation of zeolite Na-P crystals.

BET: Surface area for the prepared zeolite material was found to be $60.36\text{m}^2/\text{g}$ whereas the surface area of fly ash was only $2.89\text{m}^2/\text{g}$. The increase in surface area could be due to the formation of zeolite structure.

Adsorption studies

Effect of contact time: To study the effect of contact time of Cd^{+2} ion on adsorption behavior, two concentrations (100 and 500 mg/l) were used with a fixed adsorbent dose of 10 g/l at 298 K and at a natural pH. The contact time was varied from 15 min to 180 min for both the concentrations studied. The percentage efficiency of metal ion adsorption were calculated and plotted in (Figure 7) which indicates that the efficiency of metal adsorbed was rapid in initial stage up to 90 min but due to saturation of the active site it further decreases, it restricts further adsorption to take place. It is also observed that at the lower concentration (100 mg/l), the adsorption efficiency is high (85.3 %) as compared to the maximum efficiency of 80.33 % for 500 mg/l after 90 min of contact time. Thus the maximum contact time to attain equilibrium was experimentally found to be about 90 min.

Effect of pH: The pH of the solution was found to influence the adsorption of the adsorbate on adsorbent. The studies were conducted at adsorbate concentration of 100 mg/l, contact time (90 min) and adsorbent dose 10 g/l at 298K. pH was adjusted by adding either 0.1M HCl or 0.1M NaOH. The results obtained are presented in Figure 8, which show that adsorption of metal increases with increase in pH from 2.0 to 5.0 and after that a decrease in adsorption capacity has been observed on further increase in pH to 10.0. Maximum adsorption of cadmium metal is 85.3% at an optimum pH of 5.0. If initial pH is too high metal ion could precipitate out and this deflects the purpose of employing the sorption process as the sorption process is kinetically faster than the precipitate. The adsorption of Cd^{+2} ion becomes slower because of competitive adsorption between H^+ ions and heavy metal cation.

Effect of adsorbent dose: To examine the effect of mass of adsorbent on the adsorption of Cadmium metal, a series of adsorption experiments were carried out with different adsorbent dosage varied from 5g/l to 30g/l at an initial metal concentration of 100mg/l at natural pH and temperature 298 K. The contact time was kept 90 min and the results are shown in Figure 9. It is observed that the percentage removal efficiency of metal ion increases very slightly with increase in adsorbent dose from 5g/l to 30 g/l and after that becomes constant. The maximum efficiency at a dose of 10 g/l is 85.3 % for 100 mg/l of metal concentration respectively.

Adsorption Isotherms

Langmuir Isotherm: The adsorption of metal ion at equilibrium with increase in initial dye concentration at 298 K has been fitted in different isotherms. A perusal of data shows that the adsorption of metal ion on zeolite follows the Langmuir isotherm. Langmuir constants q_m and b are

calculated and the values of these constants are given in Table 2 along with coefficient of correlation (R^2).

Freundlich Isotherm: The equilibrium adsorption data has also been data fitted in the linear form of Freundlich isotherm model and the plots of $\log q_e$ against $\log C_e$ are linear. The values of K_F and $1/n$, calculated from intercept and slope of the plot respectively, are given in Table 2. The values of the regression coefficients indicate that the data satisfactorily follow both langmuir and freundlichmodels but the former isotherm fits the experimental data better.

Temkin Isotherm: For Temkin isotherm model isotherm q_e values were plotted against $\ln C_e$ values. Parameters obtained from the graph are given in Table 2.

Dubin-Radushkevich: Values of q_m and β were calculated according to D-R model and the coefficient of determination reflected a poor fit to the experimental equilibrium data compared to the other models used at constant temperature of 30°C .

Kinetic Studies

Pseudo First Order: The graph of pseudo first order for $\log (q_e - q_t)$ versus time (t) in minutes exhibits straight lines and confirms the adsorption process to follow first order rate kinetics. The K_{ad} value calculated from slope of the plot are given in Table 3.

Pseudo second order: To describe copper (II) adsorption, the modified pseudo-second order equation is used. A plot of t/q_t against t of equation (10) showed a linear relationship and the values obtained are shown in Table 3.

Elovich Kinetics: For Elovich analysis a linear relationship was obtained between q_t , and $\ln t$ over the whole adsorption period. It is clear that a simple elovich equation may be used to describe the kinetics of sorption of cadmium(II) on Na-P Zeolite while an expression for a fractional power function kinetic reaction failed. Table 3 lists the kinetic constants obtained from the elovich equation. It will be seen from the data that the values of a and b varied as a function of the initial Cadmium (II) concentration (C_0) and Zeolite. Although the elovich equation does not furnish any mechanistic evidence, it has proved suitable for highly heterogeneous systems of which the adsorption of cadmium (II) on to Na-P zeolite is undoubtedly such a case.

Intra Particle Diffusion: During intra particle diffusion, higher value of intercept represent greater boundary layer effect which clearly shows that rate constant increases with increase in Cd ion concentration. K_{ad} ($\text{mg/g min}^{0.5}$) value obtained from the slope of the plot of q_t (mg/g) versus $t^{0.5}$ is given in Table 3.

Conclusion

This research work concludes that zeolite synthesized from coal fly ash can be fruitfully employed as potential adsorbent for the removal of Cadmium metal ion. The pH was found to be important

factor which affects the adsorption capacity of metal ion. The removal of Cadmium metal ion is about 85.3 % at 100 mg/l with an adsorbent dose of 10 g/l and pH 5.0 at 298 K. The optimum contact time was found to be 90 min. The adsorption data was analyzed by different isotherm models. The adsorption data showed best fits in the following order based on coefficient of determination: Langmuir > Freundlich > Temkin > D-R. The suitability of Langmuir's model indicated the formation of monolayer coverage of the cadmium metal ions on the outer surface of the zeolite. The adsorption data obeyed the following order: pseudo-second order kinetics > Intra particle diffusion > Elovich kinetics > First order kinetics. The result indicates that the developed adsorbent is quite cheaper than commercially available activated carbon, while their performance is comparable.

References

1. "WHO" Guidelines for the safe use of waste water, excreta & greywater," (2006) *World Health Organization*, vol I, p.95.
2. K.Rao, M.Mohapatra, S.Anand, and P.Venkateswarlu, (2010) "Review on cadmium removal from aqueous solutions," *International Journal of Engineering, Science and Technology*, vol. 2, no. 7, pp. 81–103.
3. Ojha, K., Pradhan, N.C., & Samanta, A.N. (2004). Zeolite from fly ash synthesis and characterization, *Bull. Mater. Sci.*, 27(6), 555-564.
4. Jha, V.K., Nagae, M., Matsuda, M., & Miyake, M. (2009). Zeolite From Coal Fly Ash and Heavy metal ion removal characteristics of thus obtained zeolite X in multi-metal systems, *J. Environ. Management*, 90, 2507-2514.
5. Solanki, P., Gupta, V., & Kulshrestha, R. (2010). Synthesis of zeolite from fly ash and removal of heavy metals ions newly synthesized zeolite, *Environ. J. Chemistry*, 7(4), 1200-1205,
6. Bogomolov, J.F., Petranovsky, V.P., & Breck, W.D. (1974). Zeolite molecular sieves: New York: John Wiley and sons.
7. Kumar, P., Mal, N., Oumi, Y., Yamana, K., & Sano, T. (2001). Mesoporous Materials prepared using Coal Fly Ash as the Silicon and Aluminium Source, *Journal of Materials Chemistry*, 11, 3285-3290.
8. Jamali, H.A., Mahavi, H.A.N., & Nazmara, S. (2009). Removal of cadmium from aqueous solution by hazel nut shell. *World appl.Sci. J*, 5, 16-20.
9. Rao, M., Ramesh, A., Roa, P.C.G., & Seshaiyah, K. (2006). Removal of copper and cadmium from the aqueous solution by activated carbon derived from Ceiba pentandra hulls. *Journal of Hazardous Material*. 129(1), 123-129.
10. Erdem, E., Karapinar, N., Donat, R., (2004). The removal of heavy metal ions from natural zeolites. *J. Colloid Interface Sci.* 280-309.

11. Querol, X., Moreno, X., Umana, J.C., Alastuey, A., Hernáñez, LópezE., Soler, A., & Plana P. (2002). Synthesis of zeolites from coal fly ash an overview. *International J. of Coal Geology*, 50, 413–423.
12. Mostafa Bakr, F., Mohamed, H., Fodial, O., Ibraheem, Ali., Said-Sheikh, M., & Tarek Salama M. (2015). Controllable synthesis of Na-P zeolite and its application in calcium adsorption, *Science China Materials*, 58, 621–633.
13. Chang, H.L., & Shih, W.H. (2000). Synthesis of zeolites A and X from fly ashes and their ion exchange behaviour with cobalt ions, *Ind. Eng. Chem. Res.* 39, 4185–4191.
14. Rayalu, S.S., Bansawal, A.K., Mesharan, S.U., Labhsetwar, S., & Devotta, S. (2006). Fly ash based zeolite analysis: Versatile material for energy and environmental conservation, *Catalysis survey from Asia*, 10(2), 74–88.
15. Hui, K.S., & Chao, C.Y.H. (2006). Effects of step-change of synthesis temperature on synthesis of zeolite 4A from coal fly ash. *Microporous Mesoporous Mat.* 88, 145–151.
16. Ryu, T.G., Ryu, J.C., Choi, C.H., Kim, C.G., Yoo, S.J., Yang, H.S., & Kim, Y.H. (2006). Preparation of Na-P1 Zeolite With High Cation Exchange Capacity From Coal Fly Ash. *J. Ind. Eng. Chem.* 12(3), 401–407.
17. Chauhan, Y.P., & Taliba, M. (2012). Novel and green approach of synthesis and characterization of nano-adsorbents (zeolites) from coal fly ash: A review. *Science Review and Communications*, 2(1), 12–19.
18. Hui, K.S., Hui, K.N., & Lee, N. (2009). A novel and green approach to produce nano-porous material zeolite A and MCM -41 from coal fly ash and their application in environmental protection, *World Academy of Science, Engineering and Technology*.
19. Juan, R., Hernández, S., Andrés, J.M., & Ruiz, C. (2007). Synthesis of granular zeolitic materials with high cation exchange capacity from agglomerated coal fly ash, *Fuel*, 86, 1811–1821.
20. Koukouzas, N., Vasilatos, I., Itskos, G.S., & Moutsatsou, A. (2009). Characterisation of CFB - coal fly ash zeolite material and their potential use in waste water treatment, *Centre for Research and Technology, WOCA conference, Lexington, USA*.
21. Murayama, N., Takahashi, T., Shuku, K., Lee, H., & Shibata, J. (2008). Effect of reaction temperature on hydrothermal synthesis of potassium type zeolites from coal fly ash, *International J. Mineral Processing*. 87, 129–133.
22. Langmuir, I. (1918). The adsorption of gases on plane surfaces of glass, mica and platinum. *J. Am. Chem. Soc.* 40, 1361–1403.
23. Freundlich, H.M.F. (1906). Over the adsorption in solution. *J. Phys. Chem.* 57, 385–47.
24. Nguyen, C., Do, D.D. (2001). The Dubinin-Radushkevich equation and the underlying microscopic adsorption description. *Carbon* 39, 1327–1336.
25. Temkin, M.J., & Pyzhev, V. (1940). Kinetics of the Synthesis of Ammonia on Promoted Iron Catalysts. *Acta Physicochim.* 12, 217–222.
26. Szoastak, R. (1989). Molecular Sieves, Principle of Synthesis and Identification, *New York: Reinhold*.
27. Garg, U.K., Kaur, M.P., Garg, V.K., & Sud, D. (2007). Removal of hexavalent chromium from aqueous solution by agricultural waste biomass. *J. Hazard. Mater.* 140, 60–68.

28. Yang, X., & Al-Duri, B. (2005). Kinetic modeling of liquid-phase adsorption of reactive dyes on activated carbon. *J. Colloid Interface Sci.* 287, 25–34.
29. Hall, K.R., Eagleton, L.C., Acrivos, A., & Vermeulen, T. (1966). Pore- and Solid-Diffusion Kinetics in Fixed-Bed Adsorption under Constant-Pattern Conditions. *Ind. Eng. Chem. Fundam.* 5, 212–223.
30. Bora, M., Gangulia, J.N., & Dutta, D.K. (2000). Thermal and spectroscopic studies on the decomposition of [Ni{di(2-aminoethyl)amine}2]- and [Ni(2,20:60,200-terpyridine)2]-Montmorillonite intercalated composites. *Thermochim. Acta* 346, 169–175.
31. Aharoni, C., & Ungarish, M. (1977). Kinetics of activated chemisorption. Part 2. Theoretical models. *J. Chem. Soc. Faraday Trans.* 73, 456–464.
32. Almeida, C.A.P., Debacher, N.A., Downs, A.J., Cottet, L., & Mello, C.A.D. (2009). Removal of methylene blue from colored effluents by adsorption on montmorillonite clay. *J. Colloid Interface Sci.* 332, 46–53.
33. Bhattacharyya, K. (2003). Adsorption characteristics of the dye, Brilliant Green, on Neem leaf powder. *Dyes Pigment.* 57, 211–222.
34. Tahir, S.S., & Rauf, N. (2006). Removal of a cationic dye from aqueous solutions by adsorption onto bentonite clay. *Chemosphere.* 63, 1842–1848.
35. Rai, H.S., Bhattacharyya, M.S., Singh, J., Bansal, T.K., Vats, P., & Banerjee, U.C. (2005). Removal of dyes from the Effluent of Textile and Dyestuff Manufacturing Industry: A Review of Emerging Techniques With Reference to Biological Treatment. *Crit. Rev. Environ. Sci. Technol.* 35, 219–238.

Table 1: Chemical Constituents of the Fly Ash

Constituents	SiO ₂	Al ₂ O ₃	Fe ₂ O ₃	CaO	TiO ₂	K ₂ O	P ₂ O ₅	SO ₃	Na ₂ O	MgO	LOI
Weight %	55.26	22.75	7.12	4.1	2.95	2.14	1.65	1.58	1.23	0.63	4.1

Table 2: Langmuir, Freundlich, Temkin, Dubinin-Radushkevich isotherm parameters at 298K

ISOTHERMS	PARAMETER	UNITS	VALUES
Langmuir	q _m	mg-g ⁻¹	58.82
	B		1.133
	R ²		0.995
	R _L		0.0811
Freundlich	K _F	mg-g ⁻¹	31.55
	1/n		0.6561
	R ²		0.984
Temkin	A _t	L-mg ⁻¹	0.1113
	b _t	J-mol ⁻¹	192.2

	B_t		12.89
	R^2		0.979
Dubinin-Radushkevich	q_{DR}	$\text{mol}\cdot\text{g}^{-1}$	35.909
	B	$(\text{mol}\cdot\text{g}^{-1})^2$	6×10^{-8}
	E	$\text{KJ}\cdot\text{mol}^{-1}$	2886.75
	R^2		0.957

Table 3: Kinetic Model Parameters

Models	Parameter	Units	Values
Langergren's first order	K_{ad}	min^{-1}	0.03915
	R^2		0.969
Pseudo second order	K_2	$\text{g}\cdot\text{mg}^{-1}\cdot\text{min}^{-1}$	0.0211
	q_e	$\text{mg}\cdot\text{g}^{-1}$	8.9285
	R^2		0.998
Elovich	A	$\text{mg}\cdot\text{g}^{-1}\cdot\text{min}^{-1}$	138.033
	B	$\text{g}\cdot\text{mg}^{-1}$	1.126
	R^2		0.981
Intraparticle	K_{ad}	$\text{mg}\cdot\text{g}^{-1}\cdot\text{min}^{-0.5}$	0.302
	C		5.737
	R^2		0.987

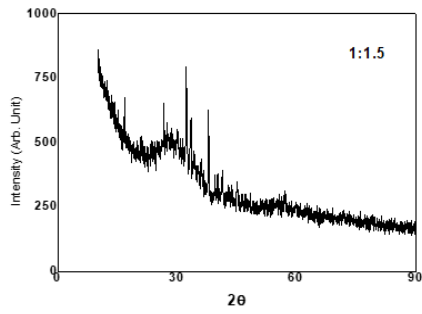


Figure 1: X-ray diffraction pattern of CFA

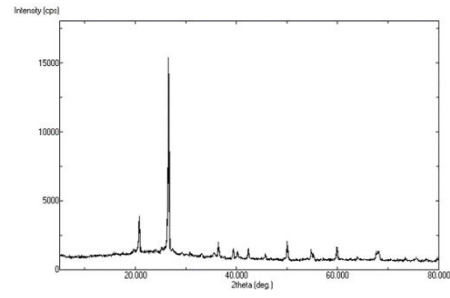


Figure 2: X-ray diffraction pattern of Zeolite

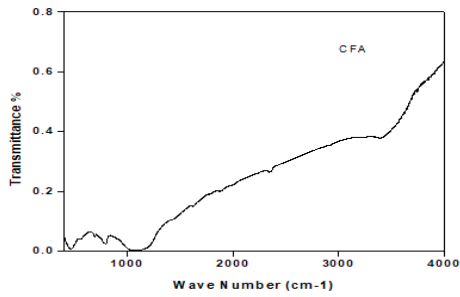


Figure 3: FTIR spectra of coal fly ash

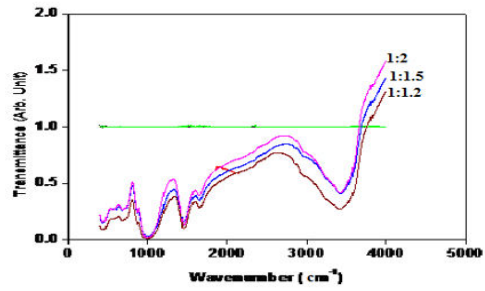


Figure 4: FTIR spectra of alkali activated CFA

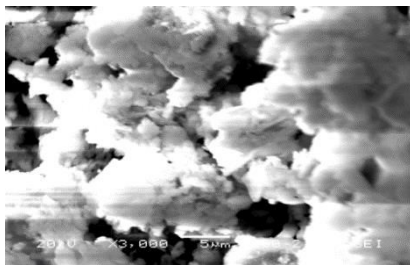


Figure 5: SEM of coal fly ash

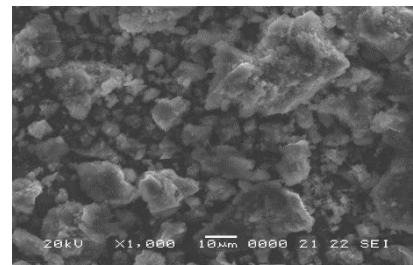


Figure 6: SEM of Zeolite

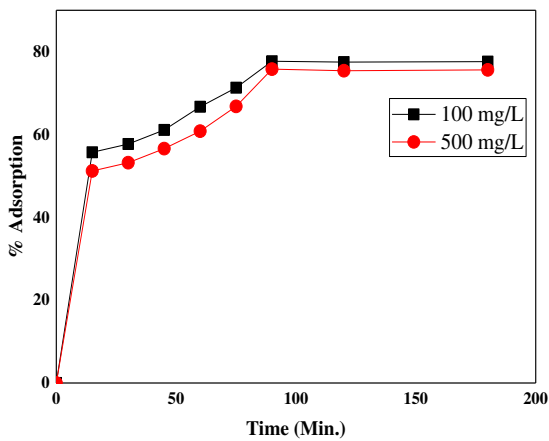


Fig: 7 Effect of contact time

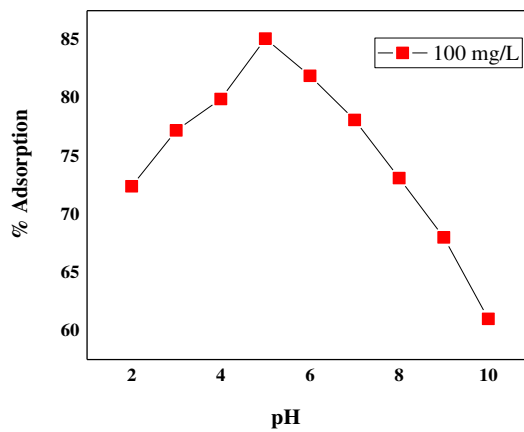


Fig: 8 Effect of pH

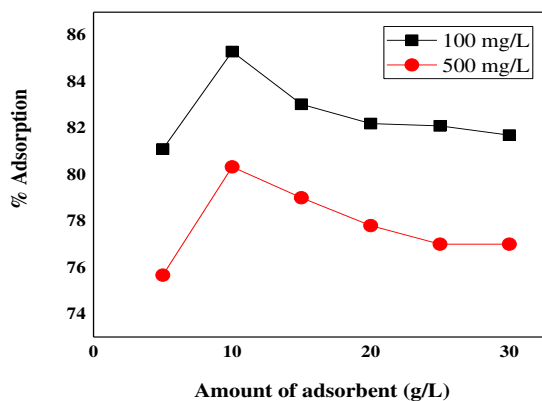


Fig: 9 Effect of Adsorbent dose

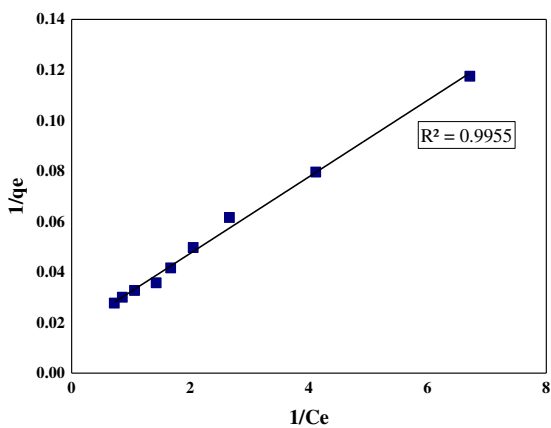


Fig: 10 Langmuir isotherm

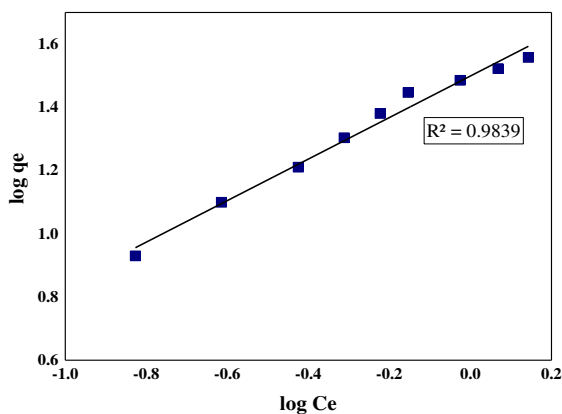


Fig: 11 Freundlich isotherm

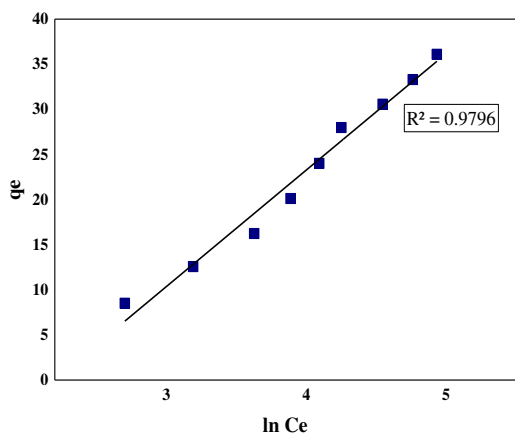


Fig: 12 Temkin isotherm

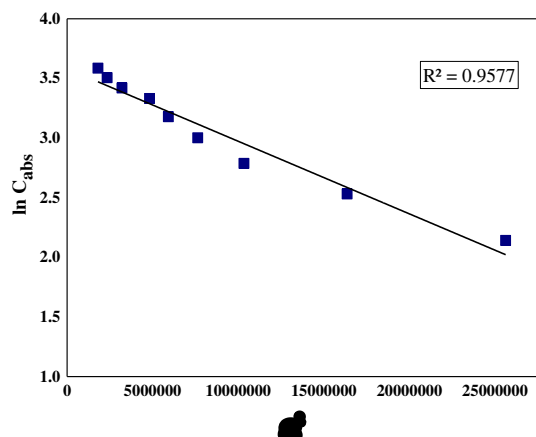


Fig: 13 Dubinin-Radushkevich isotherm

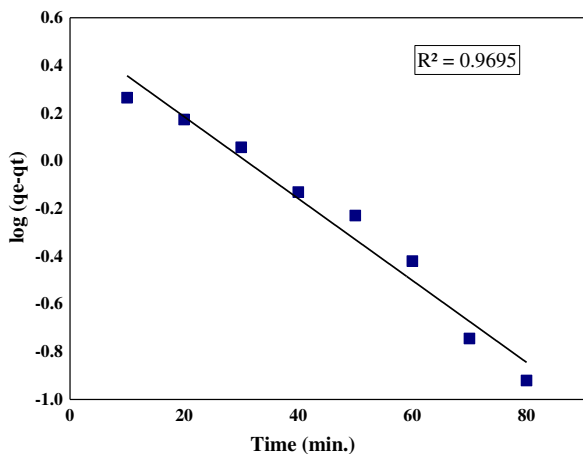


Fig: 14 Lagergren,s plot of Cd²⁺

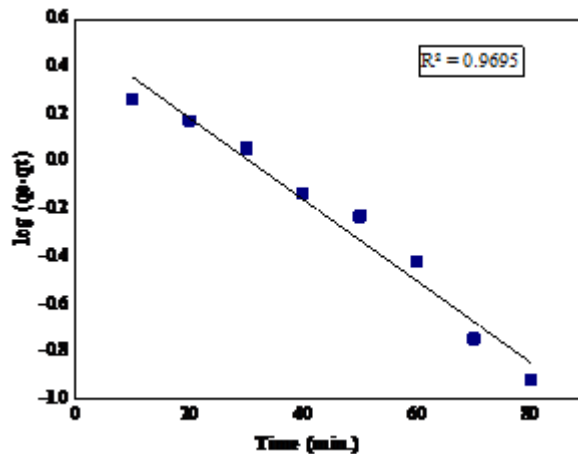


Fig: 15 Pseudo II Order

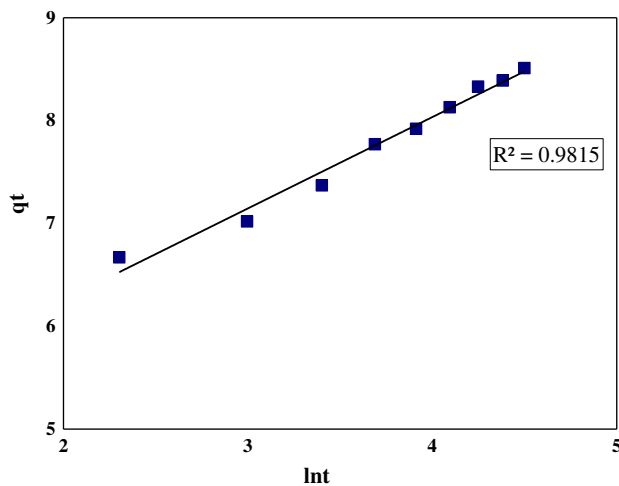


Fig: 16 Elovich model

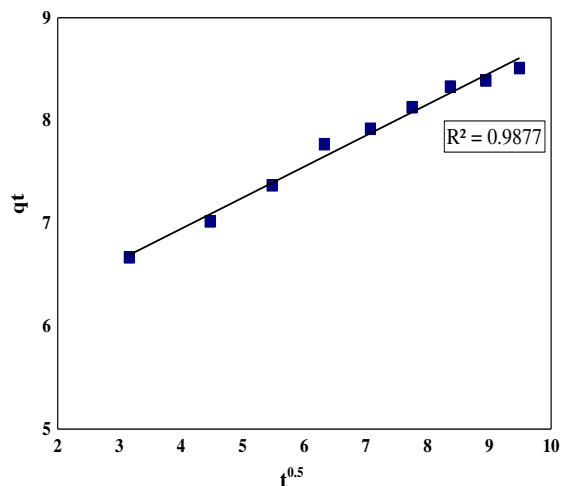


Fig: 17 Intra-Particle at 298 K